

Surface Phase Transitions Induced by Electron Mediated Adatom-Adatom Interaction

Junren Shi,¹ Biao Wu,^{1,2} X. C. Xie,^{3,4} E. W. Plummer,^{1,5} and Zhenyu Zhang^{1,5}

¹Condensed Matter Sciences Division, Oak Ridge National Laboratory, Oak Ridge, Tennessee 37831, USA

²Department of Physics, University of Texas, Austin, Texas 78712, USA

³Department of Physics, Oklahoma State University, Stillwater, Oklahoma 74078, USA

⁴International Center for Quantum Structures, Chinese Academy of Sciences, Beijing 100080, China

⁵Department of Physics, University of Tennessee, Knoxville, Tennessee 37996, USA

(Received 21 March 2003; published 15 August 2003)

We propose that the indirect adatom-adatom interaction mediated by the conduction electrons of a metallic surface is responsible for the $\sqrt{3} \times \sqrt{3} \leftrightarrow 3 \times 3$ structural phase transitions observed in Sn/Ge (111) and Pb/Ge (111). When the indirect interaction overwhelms the local stress field imposed by the substrate registry, the system suffers a phonon instability, resulting in a structural phase transition in the adlayer. Our theory is capable of explaining all the salient features of the $\sqrt{3} \times \sqrt{3} \leftrightarrow 3 \times 3$ transitions observed in Sn/Ge (111) and Pb/Ge (111), and is in principle applicable to a wide class of systems whose surfaces are metallic before the transition.

DOI: 10.1103/PhysRevLett.91.076103

PACS numbers: 68.35.Bs, 68.35.Rh, 71.45.Lr, 73.20.At

Over the years, a great deal of effort has been devoted to experimental studies of structural phase transitions at surfaces. One compelling example is the $\sqrt{3} \times \sqrt{3} \leftrightarrow 3 \times 3$ transition in the $1/3$ monolayer of Pb or Sn on Ge(111) directly observed by the scanning tunneling microscopy (STM) [1–3] (see Fig. 1). These studies have stimulated an active line of theoretical research, yet the precise nature and the underlying mechanism of such transitions are still highly controversial. The original paper attributed this transition to a charge density wave (CDW) driven by two-dimensional (2D) Fermi surface nesting [1,2]. Subsequent papers have attributed the transition to a Kohn anomaly [4], bond density waves [5], a pseudo-Jahn-Teller transition [6,7], a surface Mott insulator [8], dynamical fluctuations [9], a soft phonon [10], and most recently to disproportionation [11]. The issue becomes even more intriguing after the observation of the delicate role of defects in the transition [12,13].

In this Letter, we present a new mechanism for surface phase transitions, which places central emphasis on the indirect adatom-adatom interaction mediated by the two-dimensional conduction electrons of a metallic surface. When such adatom-adatom interaction overwhelms the local stress field imposed by the substrate, the system suffers a phonon instability, leading to a structural phase transition. The theory can explain all the salient features of the transition observed in Sn/Ge (111), including the appearance of surface CDW and the delicate role of defects. It also predicts a glassy phase in such systems.

The electron mediated adatom-adatom interaction originates from the tendency of the conduction electrons to screen external disturbances. In the adlayer systems such as Sn/Ge (111), the dangling bond electrons of the adatoms form a quasi-2D electron gas at the surface. The movement of an adatom disturbs the electron gas, which responds in the form of Friedel oscillations in its density. Such charge corrugations propagate at the surface to

reach other adatoms, thereby establishing an indirect interaction between adatoms. We note that the basic physics is similar to RKKY interaction between spins [14] and chemisorption of adatoms at metal surfaces [15–17].

We stress that the central ingredients of this picture are the existence of surface conduction electrons and their capability of coupling with the displacement of the adatoms (electron-phonon coupling). Both are evidently present in Sn/Ge (111) and Pb/Ge (111). As shown in Fig. 1, each Sn adatom bonds to three Ge substrate atoms directly under it, leaving one bond dangling. The electrons in the dangling bonds are localized in the surface and form a 2D electron system with a narrow (~ 0.5 eV) half-filled band. When an adatom is displaced, the angles between the dangling bond and its three saturated Sn-Ge bonds have to adjust accordingly, inducing a variation in the s - p hybridization of the electron states of the Sn adatom, and a corresponding change in the energy of the dangling state [18]. This process can be described by

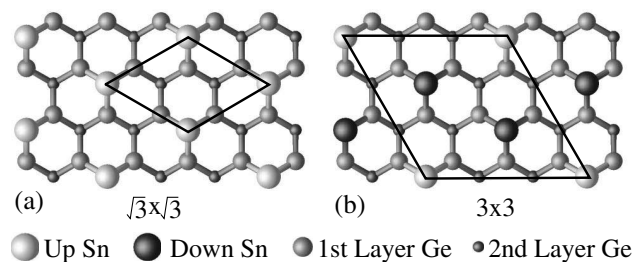


FIG. 1. Structures of $\sqrt{3} \times \sqrt{3}$ (left) and 3×3 (right) phases of Sn/Ge (111). In the experiment, one third monoatomic layer of tin was deposited onto a Ge(111) surface, and a gradual transition from the room-temperature flat $\sqrt{3} \times \sqrt{3}$ phase to the low-temperature 3×3 phase was observed [1,2]. In the new phase, one Sn adatom moves up and two move down in each 3×3 unit cell.

the Holstein electron-phonon coupling [19], where the dangling state energy of an adatom depends on its displacement as $\epsilon_d = \epsilon_0 - \beta z$, with z being the adatom displacement perpendicular to the surface, and β a positive constant, reflecting that a downward displacement induces a higher dangling state energy.

The total Hamiltonian of the system is written as

$$H = \sum_{i,s} (\epsilon_0 - \beta z_i) c_{is}^\dagger c_{is} - t \sum_{\langle ij \rangle, s} c_{is}^\dagger c_{js} + \frac{\alpha}{2} \sum_i z_i^2, \quad (1)$$

where z_i is the displacement of the adatom located at site i , and c_{is}^\dagger (c_{is}) is the creation (annihilation) operator of a dangling bond electron at site i and with spin s . The hopping constant t is between nearest neighbors and can be regarded as independent of the adatom displacement because the leading correction term is second order in z_i . The term involving α is the elastic energy of the lattice distortion caused by the displacements of the adatoms; it represents the local stress field imposed by the substrate. Here, we consider only a single electron band formed by the dangling bonds, because all other bonds of Sn are saturated and form electron bands well below the Fermi energy [20]. In Eq. (1), the higher order terms in z_i are ignored for the moment. As will become clear in later discussions, Eq. (1) is sufficient for determining the structural stability of the system, while the higher order terms are important only in stabilizing the system after the system becomes unstable.

The stability of the $\sqrt{3} \times \sqrt{3}$ phase can be examined perturbatively by expanding the total energy change up to the second order in the adatom displacements,

$$\Delta E = \frac{\alpha}{2} \sum_i z_i^2 - \beta \langle n \rangle \sum_i z_i - \frac{1}{4} \sum_{ij} J_{ij} (z_i - z_j)^2, \quad (2)$$

where $\langle n \rangle$ is the average electron number for each adatom, and J_{ij} are the coupling coefficients for the adatom-adatom interaction. In the continuum limit, we have

$$J_{ij} = 8\beta^2 \sum_{\epsilon_q < \epsilon_F} \sum_{\epsilon_k > \epsilon_F} \frac{\exp[-i(\mathbf{q} - \mathbf{k}) \cdot (\mathbf{R}_i - \mathbf{R}_j)]}{\epsilon_q - \epsilon_k} \approx \frac{8n^2 \beta^2}{\epsilon_F} F(k_F |\mathbf{R}_i - \mathbf{R}_j|), \quad (3)$$

where ϵ_q (ϵ_k) is the energy dispersion of the electron band, ϵ_F is the Fermi energy relative to the band bottom, and contains implicitly the hopping constant t . The coefficients J_{ij} are the same as for the 2D RKKY coupling [21], and are oscillatory spatially with an asymptotic dependence of $-\sin(2k_F r)/r^2$, as shown in Fig. 2(a). In the case of the $\sqrt{3} \times \sqrt{3}$ structure of Sn/Ge (111), the coupling between the nearest neighbors is positive; therefore, two nearest neighboring adatoms tend to displace in opposite directions.

Keeping only the interacting terms between nearest neighbors, we can reduce Eq. (2) to

$$\Delta E = \frac{1}{2} (\alpha - 6J_1) \sum_i \tilde{z}_i^2 + \frac{J_1}{2} \sum_{\langle ij \rangle} \tilde{z}_i \tilde{z}_j, \quad (4)$$

where $\tilde{z}_i = z_i - \beta/(\alpha \langle n \rangle)$. This equation shares the same form as the phenomenological charge compensate model (CCM) [22], which has been shown to be capable of interpreting most of the STM images. Our theory thus provides the microscopic mechanism behind the success of the CCM model.

From Eq. (4), it is evident that the system becomes unstable against adatom displacements when the elastic restoring force is weak. This can be illustrated with the phonon dispersion of Eq. (4) [10]:

$$\omega^2 = \alpha - 6J_1 + J_1 \sum_l \cos(\mathbf{k} \cdot \mathbf{R}_l), \quad (5)$$

where the sum is over six nearest neighbors. When $\alpha/J_1 < 9$, ω becomes imaginary for certain \mathbf{k} vectors [Fig. 2(b)], indicating that the corresponding phonon modes become unstable (phonon catastrophe) and the system is driven into new phases. Note that the soft phonon picture suggested in Ref. [10] is a very special case of our model, occurring only when α/J_1 is exactly equal to 9. Furthermore, the phonon instability established here does not require any special properties of the Fermi surface such as the Fermi surface nesting, nor

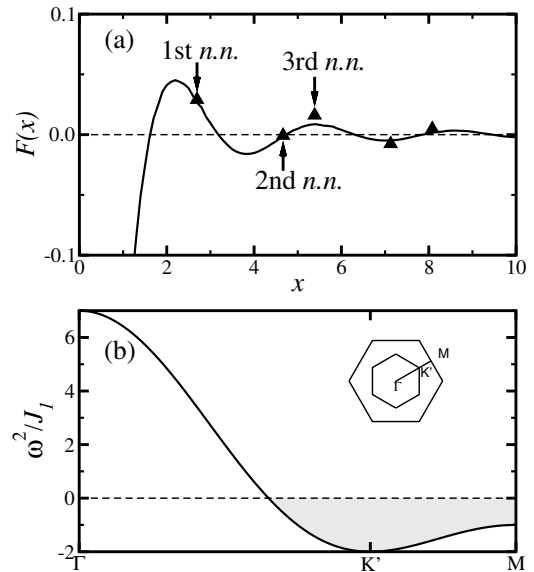


FIG. 2. (a) $F(x)$ in Eq. (3) (as a comparison, the triangles are the results of tight-binding calculations up to the fifth nearest neighbors for the $\sqrt{3} \times \sqrt{3}$ structure). In this system, the Fermi momentum $k_F \approx \sqrt{2\pi\rho} = \sqrt{4\pi}/(3^{1/4}a)$, where ρ is the density of the surface electrons and a is the lattice constant. (b) Phonon dispersion [Eq. (4)] along the direction ΓM shown in the inset, with $\alpha/J_1 = 7$. The shaded area indicates the unstable phonon modes, of which the most unstable K' mode defines the 3×3 periodicity.

does it rely on the electron-electron interaction, which is the focus of many earlier efforts with little success [8,23].

Higher order terms become important when the system enters the unstable regime. Microscopically, those terms may arise from a variety of sources, such as anharmonicity in the elastic energy, finite width of the electron band, higher order terms in expansions of the site energy, and the hopping constant t . The precise form of these higher order terms may affect the quantitative details of the phase transition, such as the amplitudes of adatom displacements and preference among the nearly degenerate ground states, but the occurrence and nature of the transition is totally determined by the intrinsic instability represented in Eq. (4). For this reason and simplicity, we assume that the higher order terms mainly come from the anharmonic terms of the on-site elastic energy,

$$-\frac{\delta}{3}\sum_i \tilde{z}_i^3 + \frac{\gamma}{4}\sum_i \tilde{z}_i^4, \quad (6)$$

where $\delta > 0$ and $\gamma > 0$. δ is positive, because displacing an adatom out of the surface weakens the bond strengths between the adatom and the substrate atoms.

By adding those higher order terms into Eq. (4), we can determine the stable configurations. The numerical results are shown in Fig. 3. The ratio α/J_1 determines the phase transition. When $\alpha/J_1 \geq 9$, the ground state is the flat $\sqrt{3} \times \sqrt{3}$ phase. When $6 \leq \alpha/J_1 < 9$, the ground state is the 3×3 phase in the one-up–two-down configuration: In each unit cell of the 3×3 lattice, one Sn adatom moves up (z_\uparrow), while the other two move down (z_\downarrow), and the displacements satisfy $z_\uparrow \approx 2|z_\downarrow|$. The nearly degenerate one-down–two-up configuration has a higher energy due to the cubic term in Eq. (6). Such 3×3 patterns were also observed experimentally [7,24]. Note that the 3×3 structure corresponds to the most unstable phonon mode in Eq. (5) [see Fig. 2(b)].

When $\alpha/J_1 < 6$, the system shows kinked-line configuration and behaves similar to a glass [25]. Starting with random initial configurations, we always end up with a metastable disordered structure as typified in

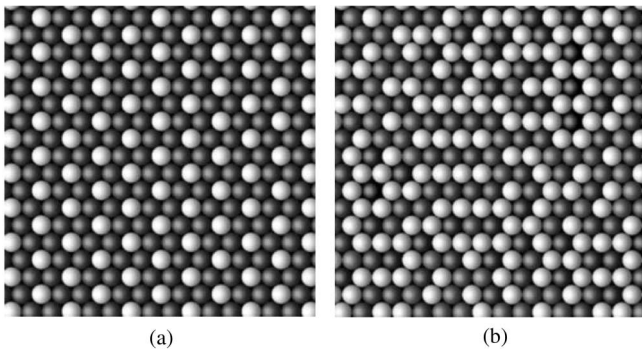


FIG. 3. Schematic images of the stable configurations for different parameter regimes. (a) 3×3 phase for $6 \leq \alpha/J_1 < 9$; (b) kinked-line phase for $\alpha/J_1 < 6$.

Fig. 3(b), instead of the true ground state 3×3 . We expect a similar behavior in a realistic experiment with finite cooling rates: The system is trapped in one of the metastable states, showing a disordered configuration. Such behavior is directly related to the property of the single body potential of an adatom,

$$\frac{1}{2}(\alpha - 6J_1)\tilde{z}_i^2 - \frac{\delta}{3}\tilde{z}_i^3 + \frac{\gamma}{4}\tilde{z}_i^4, \quad (7)$$

which develops a double-well shape when $\alpha/J_1 < 6$. As a result, the present model can be mapped onto an Ising antiferromagnet by considering the displacement \tilde{z}_i taking discrete values at the local minima of the double-well potential. Such an Ising antiferromagnet on a triangular lattice is known to have an exponentially large number of degenerate ground states [26].

As quantitative estimates, for Sn/Ge we have $\alpha = M_{\text{Sn}}\omega_{\text{ph}}^2 \sim 1.8 \text{ eV}/\text{\AA}^2$ [10]; $\epsilon_F \sim 0.3 \text{ eV}$ [20], and β is of the order of $1 \text{ eV}/\text{\AA}$ [8]. Based on Eq. (3), we get $J_1 \sim 0.8 \text{ eV}/\text{\AA}^2$ and $\alpha/J_1 \sim 2$. This result indicates that the electron mediated adatom-adatom interaction is indeed strong enough to induce the structural phase transition for Sn/Ge. For Sn/Si, we have larger values of α and ϵ_F because of stronger Sn-Si bond strength and smaller Sn-Sn distance. Both suggest a larger value of α/J_1 , which is qualitatively consistent with the experimental observations that the $\sqrt{3} \times \sqrt{3} \leftrightarrow 3 \times 3$ transition can take place in Sn/Ge and Pb/Ge but not in Sn/Si.

The structural phase transition manifests itself by an accompanying charge density wave, as observed experimentally [1,2]. Following the Hellmann-Feynman theorem, we obtain the total force acting on an adatom $F_i = \alpha z_i - \beta \langle n_i \rangle + \mathcal{O}(z^3)$. Setting $F_i = 0$ in equilibrium, we have $\langle n_i \rangle = \langle n \rangle + (\alpha/\beta)\tilde{z}_i + \mathcal{O}(\tilde{z}^3)$, showing that adatoms displaced upward gain electrons while those downward lose electrons. The Coulomb energy induced by such charge transfer renormalizes the parameters in Eq. (2) as $\alpha \rightarrow \alpha + (\alpha/\beta)^2 U$ and $J_{ij} \rightarrow J_{ij} + (\alpha/\beta)^2 V_{ij}$, where U and V_{ij} are the on-site and off-site Coulomb repulsion energy, respectively. For Sn/Ge, we take $U \sim 1 \text{ eV}$ [8] and the worst case scenario $V_{ij} = 0$; this leads to $\alpha/J_1 \sim 6$, still in the parameter regime for the existence of the structural instability.

We now study the finite temperature behavior of the system by applying the Metropolis Monte Carlo algorithm [27] to the effective classical Hamiltonian shown in Eq. (4) along with Eq. (6). We find that the transition between the $\sqrt{3} \times \sqrt{3}$ phase and the 3×3 phase is of second order with a sharply defined boundary, as shown in Fig. 4. There exists another boundary between the glassy phase and the 3×3 phase, which is the result of the glassy states at $T = 0$ when $\alpha/J_1 < 6$. As is typical in a glassy system, the boundary of the glassy phase is not well defined. The detailed behavior of the $\sqrt{3} \times \sqrt{3} \leftrightarrow 3 \times 3$ phase transition along the temperature axis is

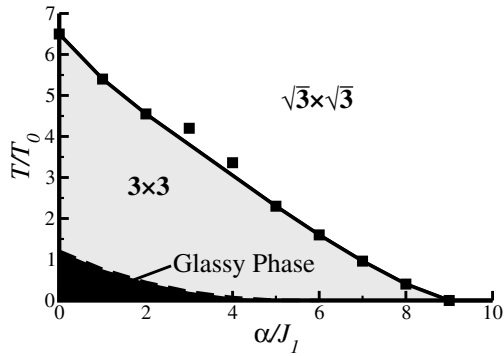


FIG. 4. Phase diagram of the system. The boundary between the glassy phase and the 3×3 ground state is not well defined as indicated with the dashed line. $T_0 = J_1^2/\gamma$, $\delta = 0$.

shown in Fig. 5. The order parameter is chosen as the mean square corrugation of the thermoaverage positions of adatoms [22]. The defect-free system clearly shows a second-order transition from the 3×3 phase to the $\sqrt{3} \times \sqrt{3}$ phase as seen in Fig. 5, where the temperature dependence of the order parameter is well fitted by $A(1 - T/T_c)^{1/2}$. This is different from the prediction of the Ginzburg-Landau-type theories such as the CCM, where the critical behavior follows $|1 - T/T_c|$ [22].

Figure 5 also shows that the sharp phase transition is blurred by the presence of a very low concentration of substitutional defects, explaining the experimental observation that the transition is gradual. In our calculations, the defect is simulated by a constant displacement, $\Delta z = -\Delta\epsilon/\beta$, where $\Delta\epsilon$ is the site energy difference between a Ge substitutional defect and a Sn adatom [4]. Just as in the experiments [12,22], our simulations show that each defect induces a local 3×3 patch above T_c , and the size of

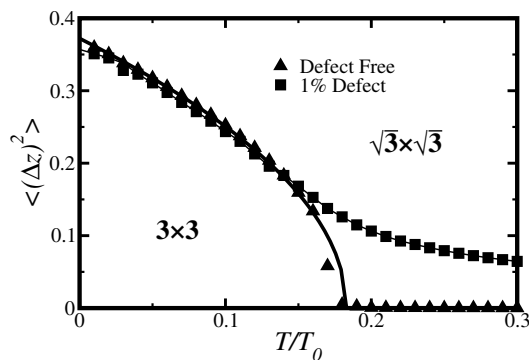


FIG. 5. Temperature dependence of the order parameter for the defect-free system and the system with 1% defect. The thick solid line shows the function $A(1 - T/T_c)^{1/2}$ with $T_c/T_0 = 0.18$, $T_0 = J_1^2/\gamma$. The parameters are $\alpha/J_1 = 8.5$, $J_1 = 1$, $\gamma = 1.0$, and $\delta = 0.1$, with a simulation system size of 99×99 .

each individual 3×3 patch decreases gradually with the increasing temperature.

In conclusion, we have presented a complete theory to understand the surface phase transitions observed in Sn/Ge (111) and Pb/Ge (111). The central ingredients of the theory, namely, the electron mediated indirect interaction and the resulting phonon instability, are conceptually very general, and applicable to a wide class of systems whose surfaces are metallic before the transition.

We acknowledge discussions with A. Melechko, H. Weitering, Ismail, Jiandi Zhang, A. Chernyshev, and Q. Niu. This work was supported in part by the LDRD of ORNL, managed by UT-Battelle, LLC for the USDOE (DE-AC05-00OR22725). It was also supported by the NSF DMR-0105232 (E. W. P.), DMR-0071893 (B. W. and Z. Z.), and the USDOE DE-FG03-01ER45687 (X. C. X.).

- [1] J. M. Carpinelli, H. H. Weitering, E. W. Plummer, and R. Stumpf, *Nature (London)* **381**, 398 (1996).
- [2] J. M. Carpinelli *et al.*, *Phys. Rev. Lett.* **79**, 2859 (1997).
- [3] L. Petersen, Ismail, and E. W. Plummer, *Prog. Surf. Sci.* **71**, 1 (2002).
- [4] T.-C. Chiang, M. Y. Chou, T. Kidd, and T. Miller, *J. Phys. Condens. Matter* **14**, R1 (2002).
- [5] S. de Gironcoli *et al.*, *Surf. Sci.* **454–456**, 172 (2000).
- [6] O. Bunk *et al.*, *Phys. Rev. Lett.* **83**, 2226 (1999).
- [7] J. Zhang *et al.*, *Phys. Rev. B* **60**, 2860 (1999).
- [8] G. Santoro, S. Scandolo, and E. Tosatti, *Phys. Rev. B* **59**, 1891 (1999).
- [9] J. Avila *et al.*, *Phys. Rev. Lett.* **82**, 442 (1999).
- [10] R. Pérez, J. Ortega, and F. Flores, *Phys. Rev. Lett.* **86**, 4891 (2001).
- [11] G. Ballabio *et al.*, *Phys. Rev. Lett.* **89**, 126803 (2002).
- [12] H. H. Weitering *et al.*, *Science* **285**, 2107 (1999).
- [13] A. V. Melechko, J. Braun, H. H. Weitering, and E. W. Plummer, *Phys. Rev. B* **61**, 2235 (2000).
- [14] M. A. Ruderman and C. Kittel, *Phys. Rev.* **96**, 99 (1954).
- [15] T. L. Einstein and J. R. Schrieffer, *Phys. Rev. B* **7**, 3629 (1973).
- [16] K. H. Lau and W. Kohn, *Surf. Sci.* **75**, 69 (1978).
- [17] J. Repp *et al.*, *Phys. Rev. Lett.* **85**, 2981 (2000).
- [18] W. A. Harrison, *Electronic Structure and the Properties of Solids* (Dover, New York, 1989), p. 235.
- [19] T. Holstein, *Ann. Phys. (N.Y.)* **8**, 325 (1959).
- [20] G. Ballabio, S. Scandolo, and E. Tosatti, *Phys. Rev. B* **61**, R13 345 (2000).
- [21] B. Fischer and M. W. Klein, *Phys. Rev. B* **11**, 2025 (1975).
- [22] A. V. Melechko *et al.*, *Phys. Rev. B* **64**, 235424 (2001).
- [23] G. Santoro, S. Scandolo, and E. Tosatti, *Comput. Mater. Sci.* **20**, 343 (2001).
- [24] L. Petaccia *et al.*, *Phys. Rev. B* **63**, 115406 (2001).
- [25] C. A. Angell, *Science* **267**, 1924 (1995).
- [26] G. H. Wannier, *Phys. Rev.* **79**, 357 (1950).
- [27] M. Metropolis *et al.*, *J. Chem. Phys.* **21**, 1807 (1953).